JOURNAL OF MATERIALS SCIENCE 31 (1996) 5505–5511

Preparation of zirconia powders from molten nitrites and nitrates

Y. DU, D. INMAN
Department of Materials, Imperial College, London SW7 2BP, UK

Finely dispersed ZrO_2 powders with high purity have been prepared by the reactions of $Zr(SO_4)_2$ in molten nitrites and nitrates. The effects of the starting materials of α-$Zr(SO_4)_2$ and β-$Zr(SO_4)_2$, the different nitrate and nitrite melts, and reaction conditions such as temperature and time, on the structure and crystallite size of the ZrO_2 powders produced were investigated. The processing of the prepared powders was also studied under different conditions; the results showed that very fine ZrO_2 powders with soft agglomeration could be produced if the proper treatment of the powders was applied.

1. Introduction

The preparation of finely divided ZrO_2 powders has been studied largely in aqueous solutions. However, the molten salt method as a new relatively low-temperature route has just begun to be studied [1, 2]. Earlier, Kerridge and Cancela Rey [3] investigated the reaction of $Zr(SO_4)_2$ in $LiNO_3/KNO_3$ eutectic. It was shown that the reaction took place at about 200 °C with the precipitation of ZrO_2 powders and that when the melt contained Lux-Flood bases (Na_2O_2, Na_2O, NaOH), the reaction occurred at even lower temperatures. However, the properties of the precipitated powders, for instance the size, were not stated. Later, Finch and Belcher [4] explored the growth of a monoclinic macrocrystalline ZrO_2 by the hydrolysis of LiF/NaF eutectic containing ZrF_4 at relatively high temperatures of 650–800 °C. Durand and co-workers [1, 2] investigated the reactions of metallic salts with molten alkali nitrates to produce pure or stabilized ZrO_2, for example, yttria-stabilized ZrO_2. Al-Raihani *et al.* [5] further studied the reactions in different nitrate and nitrite melts and characterized the powder products. Recently, we studied the kinetics and mechanism of the reactions of $Zr(SO_4)_2$ in molten $NaNO_3/KNO_3$ and $NaNO_2/KNO_2$ eutectics and found that the differences in kinetics and mechanism resulted in differences of the properties of the precipitated powders such as the structure and crystallite size [6]. On the basis of the results that the differences in powder properties were probably caused by the differences in nitrites and nitrates in terms of acidity/basicity, further studies were performed on the acidic/basic effects on the properties of the ZrO_2 powders produced [7] including the structure, phase composition and crystallite size. As a result of this study, it was surmised that the chemistry of the molten salt solution plays a key role in determining the structure and crystallite size of the powders precipitated.

However, the effects of the reaction conditions, such as the starting materials, temperature and time, and the processing methods, which has been shown to be important for powders agglomeration [8], on the preparation and properties of the ZrO_2 powders yielded have been little studied especially in the nitrite melts, which are more basic than nitrate melts from the Lux–Flood acid–base theory [6]. The aim of this study was to undertake this research in molten nitrites and nitrates in order to find the best conditions to produce ideal ZrO_2 powders.

2. Experimental procedure

Previous researchers employed Bear's method [9] to dehydrate zirconium (IV) sulphate tetrahydrate ($Zr(SO_4)_2 \cdot 4H_2O$) using concentrated sulphuric acid followed by ignition at about 350 °C for about 8 h. By this method α-$Zr(SO_4)_2$, which is the stable form of anhydrous $Zr(SO_4)_2$ could be obtained [10]. Considering that Bear's method is not desirable in practice because the use of concentrated sulphuric acid, which gives rise to a series of problems such as the danger in operation, higher cost and longer time in dehydration, it is hoped to replace this method. Therefore, another method based on a simple heating of $Zr(SO_4)_2 \cdot 4H_2O$ to 350 °C for 2 h was also used in order to compare the effects of both dehydration routes on the preparation of ZrO_2 powders. In this way, the metastable β-$Zr(SO_4)_2$ or γ-$Zr(SO_4)_2$ would be prepared [11].

The eutectics of $LiNO_3/KNO_3$ (m.p. 132 °C), $NaNO_3/KNO_3$ (m.p. 220 °C) and $NaNO_2/KNO_2$ (m.p. 220 °C) were prepared using dried chemicals in the mole ratios of 43:57, 50:50, and 65:35, respectively, by heating the eutectic mixtures at 50 °C above their melting points for half an hour.

The preparation of ZrO_2 powders employed a Pyrex tube in a vertical furnace, as described by Al-Raihani *et al.* [5].

The molten salt containing the precipitated powders was cooled naturally or by pouring into a ceramic dish soon after the reaction. Then distilled water was

0022-2461

applied to dissolve the melt and remove the anions such as NO_3^-, NO_2^- and SO_4^{2-}. The precipitated powders were extracted by vacuum filtration. Sometimes an MSE 10 high-temperature centrifuge was utilized to separate precipitates from liquids. This procedure was repeated a number of times until no anions, for example SO_4^{2-}, NO_3^- and NO_2^-, could be detected [12]. In order to obtain soft or non-agglomerated powders, the following processing methods were also utilized during the washing procedure. The first utilized dilute H_2SO_4 during water washing. The second employed isopropyl alcohol after water washing and the third used a Jencons high-intensity ultrasonic processor (600 W) to break the aggregates and disperse the particles.

A Philips PW-1050 X-ray diffractometer (XRD) was employed to identify the structure and estimate the crystallite size according to Scherer's equation [13]. Chemical analysis was performed with a Perkin–Elmer 2380 atomic absorption spectroscope (AA) and the morphologies of the powders such as the particle size were measured by a high-resolution Philips EM 301 (100 kV) transmission electron microscope (TEM).

3. Results and discussion

3.1. Preparation of ZrO_2 in the $NaNO_2$–KNO_2 melt

The preparation of ZrO_2 powders by the reaction of $Zr(SO_4)_2$ with $NaNO_2$–KNO_2 was conducted under different conditions and the results are listed in Table I. It can be seen from the first group of experiments, all using programme 1 (experiments 1–4, Table I), that powders of tetragonal ZrO_2 with almost the same crystallite size were prepared, when using either the $NaNO_2$–KNO_2 eutectic, prepared by melting the eutectic mixture at 270 °C, 50 °C above its melting point, or using the simple eutectic mixture without melting before the experiments. In addition, there were no differences in either structure or crystallite size when using α-$Zr(SO_4)_2$ or β-$Zr(SO_4)_2$ as starting materials under the same conditions. These results indicate that the employment of either eutectic or eutectic mixture as solvents, and α-$Zr(SO_4)_2$ or β-$Zr(SO_4)_2$ as starting materials do not affect the final ZrO_2 powder produced either in its structure or crystallite size. Therefore, it is not necessary to prepare $NaNO_2$–KNO_2 eutectic by melting the mixture in advance and α-$Zr(SO_4)_2$ by Bear's method, which can involve danger, higher cost and longer time in the process of dehydration because of using concentrated H_2SO_4. The elimination of these hindrances leads to an improvement in the process which is very desirable in practice, especially in industry, because the production process is much simpler and therefore the cost can be greatly reduced.

TABLE II Temperature programmes

Programme	Temp. range (°C)	Heating rate (°C h^{-1})	Holding time (min)	Adding temp. of $Zr(SO_4)_2$ (°C)
p1	20–450	300	30	Room temp.
p2	20–450	300	30	320
p3	20–450	150	90	Room temp.
p4	20–450	150	300	Room temp.

Programme 2, where the starting materials (α-$Zr(SO_4)_2$ and β-$Zr(SO_4)_2$) were added at 320 °C, approximately 100 °C above the melting point of the $NaNO_2$–KNO_2 eutectic and 150 °C above the reaction starting temperature [6], was used in experiments 5 and 6 (Table I) in order to allow the reaction to occur at a higher temperature. This caused the reaction to take place much more rapidly and to finish almost within a minute. On further heating, very little gas evolved. As a result the crystallite size was reduced. This is in agreement with the results [6, 7] which reveals that faster reaction and shorter reaction time can lead to a reduction of the crystallite size. The reduction of crystallite size resulting from faster reaction at higher temperatures might be explained because it allowed the formation of many more nuclei at an early stage of reaction in a very short duration and constrained the growth of these nuclei to a short time. In addition, the same crystallite size and phase obtained demonstrated again that the employment of either α-$Zr(SO_4)_2$ or β-$Zr(SO_4)_2$ as the starting materials to produce zirconia leads to the same results.

TABLE I Reaction results of $Zr(SO_4)_2$ in $NaNO_2$–KNO_2

No.	Melt	Temp. programme[a]	Starting material	Phase	Crystallite size (nm)
1	Eut[b]	p1	α-$Zr(SO_4)_2$	T[d]	3.8
2	Mix[c]	p1	α-$Zr(SO_4)_2$	T	3.8
3	Mix	p1	β-$Zr(SO_4)_2$	T	3.8
4	Eut	p1	β-$Zr(SO_4)_2$	T	3.9
5	Mix	p2	α-$Zr(SO_4)_2$	T	3.5
6	Mix	p2	β-$Zr(SO_4)_2$	T	3.5
7	Eut	p3	β-$Zr(SO_4)_2$	T	4.6
8	Mix	p3	α-$Zr(SO_4)_2$	T	4.7
9	Mix	p4	α-$Zr(SO_4)_2$	T	6.0

[a] See Table II.
[b] Eutectic of $NaNO_2$–KNO_2 prepared by melting its mixture in advance.
[c] Simple eutectic mixture of $NaNO_2$–KNO_2 without melting before experiments.
[d] Tetragonal.

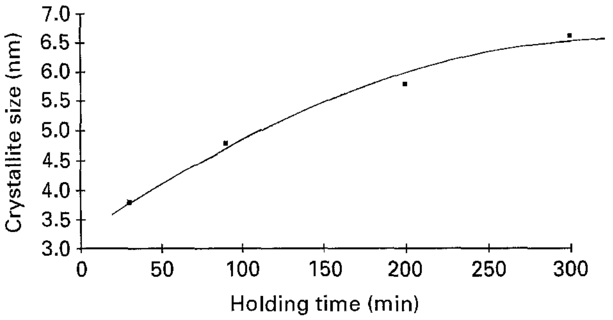

Figure 1 Relationship between crystallite size and holding time at 450 °C.

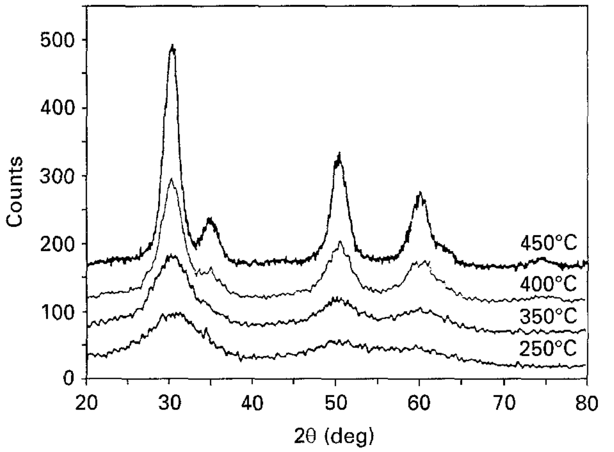

Figure 2 XRD patterns showing the effect of temperatures on the structures of ZrO_2 powder.

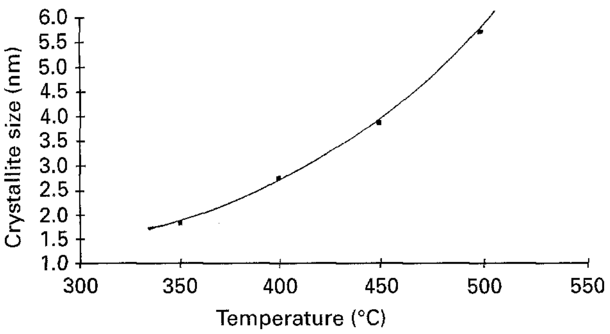

Figure 3 Crystallite size of powders and temperatures (holding for 90 min) of reaction.

Programme 3 (Table I) used a lower heating rate and longer holding time (90 min) at the highest temperature (450 °C). Both of these led to longer reaction times. Experiments 7 and 8, which used this programme, resulted in an increase of crystallite size. Experiment 9 (Table I), which further increased the holding time (300 min), indicated that the crystallite size increased still further. The lower heating rate allowed the reactions to take place at lower temperatures for a longer time and therefore at lower reaction rates. This would lead to fewer nuclei forming at the early stage of the reaction. On the other hand, the longer reaction time would allow the nuclei to grow. This results in larger crystallite size powders being produced compared to the powders obtained at higher reaction rates and shorter reaction times (experiments 1–6, Table I). Experiments with different holding times at 450 °C were conducted and the effects on crystallite size of ZrO_2 powders produced is shown in Fig. 1.

Finally, the influence of temperature on the ZrO_2 powders produced was investigated. As can be seen from Fig. 2, which shows the XRD results of ZrO_2 powders prepared from 250–450 °C (at each temperature holding for 90 min), ZrO_2 powders changed from poorly or non-crystalline to crystalline with increasing reaction temperature.

Below 350 °C, the ZrO_2 powder was poorly crystalline or amorphous, whereas above 400 °C it became crystalline. The sharper XRD peaks at higher temperatures also indicate that the crystallite size increases with increasing temperature. This can be explained on the basis that at low temperatures crystal growth and lattice movement were slow, therefore the newly formed powders were very fine and could not become properly crystalline. However, at higher temperatures the faster lattice movement and crystal growth would make these very fine powders become larger and crystalline. In addition, all these reactions occurred under the same conditions at the early stage where the formation of nuclei takes place. Therefore, the increase in temperature at the end point, whilst not influencing the formation of nuclei, did prolong the reaction time and, thus, the growth time because all the experiments were carried out at the same heating rate. In addition, the crystal growth rate was increased. In this way, the experiments at higher temperatures had longer growth times and faster growth rate. The crystallite size calculated according to Scherrer's equation [13] at different temperatures (holding for 90 min) is schematically shown in Fig. 3.

All of these experimental results illustrate that the ZrO_2 powders produced consisted of the single tetragonal phase with a crystallite size less than 10 nm in the $NaNO_2$–KNO_2 system, whether using α-$Zr(SO_4)_2$ or β-$Zr(SO_4)_2$ as the starting material. The higher basicity and the reaction kinetics and mechanism are probably responsible for these [6, 7].

3.2. Preparation of ZrO_2 in nitrate systems

The XRD patterns of ZrO_2 powders produced by the reaction of $Zr(SO_4)_2$ in different nitrate systems are shown in Fig. 4 and the preparative results under different conditions are listed in Table III.

In contrast to the synthesis of ZrO_2 powders in the $NaNO_2$–KNO_2 system where the tetragonal phase was produced, all the powders produced under different reaction conditions (i.e. temperatures, times, starting materials, solvents) in different nitrate systems consisted of mixtures of the monoclinic and tetragonal phases. The phase compositions, calculated according to the ratio of peak intensities $[I(1\,1\,1)_T/I(1\,1\,1)_T + I(1\,1\,\bar{1})_M + I(1\,1\,1)_M]$ [7], however, were different as demonstrated by the intensities of relative peaks (Fig. 4, 2θ around 28°–31°). The crystallite sizes were in the range of 10–20 nm. Although the sizes were still very fine, they were larger than those of the powders produced in the $NaNO_2$–KNO_2 system. The increase

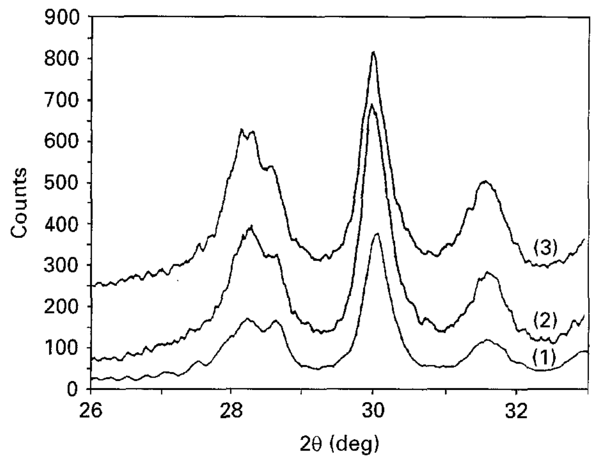

Figure 4 XRD patterns of ZrO_2 prepared in the nitrate systems. (1) β-$Zr(SO_4)_2$ + $LiNO_3$–KNO_3; (2) β-$Zr(SO_4)_2$ + $NaNO_3$; (3) β-$Zr(SO_4)_2 \cdot 4H_2O$ + $LiNO_3$–KNO_3.

of crystallite size was likely to be caused by slower reactions in nitrate systems [6] resulting in the formation of fewer nuclei but greater nucleus growth. The mixture of the monoclinic and tetragonal phases may be caused by the presence of multiple reaction stages or side reactions [6].

The structure of ZrO_2 yielded in the $NaNO_3$–KNO_3 melt at different temperatures showed a similar trend to the nitrite system (Fig. 2), i.e. it changed from poorly crystalline or amorphous at lower temperatures ($\leqslant$ 300 °C) to crystalline at higher temperatures ($\geqslant$ 400 °C) and the crystallite size increased with increasing reaction time (Table III, nos 5, 8) and temperature (Table III, nos 7, 8).

Comparing experiments 3 and 5 in Table III, it was found that the powders prepared by the addition of $Zr(SO_4)_2$ at 320 °C to the $NaNO_3$–KNO_3 melt did not decrease the crystallite size, although the reaction time was decreased. This is probably because the reaction was slow at low temperature in the $NaNO_3$–KNO_3 melt [6] and its influence on crystallite size was very small. Another possible reason could be that the ZrO_2 produced was mainly in the stage of forming nuclei and the nucleus growth was less important at low temperatures. The formation of poorly crystalline or amorphous structures at low temperature possibly indicates that the crystal growth occurs mainly at higher temperatures. Finally, error in the calculation from XRD peak broadening could also be responsible for it.

A similar explanation can be applied to the results indicating the same crystallite size for ZrO_2 produced by using $Zr(SO_4)_2 \cdot 4H_2O$ and β-$Zr(SO_4)_2$ (Table III, nos 4, 5) as the starting materials under the same conditions. The evolution of H_2O occurred below 350 °C [5] and the effect on the crystallite size below this temperature was very small.

The crystallite size of ZrO_2 powders produced in different melts (Table III, nos 1, 2, 3) under the same conditions decreased with decreasing melting point. The differences are probably caused by their differences in basicity [6, 7]. In addition to resulting in kinetics and mechanism differences in the reactions, and differences in phase composition, the lower basicity in the nitrate systems can result in quicker reaction and smaller crystallite size of the ZrO_2 powders produced. The acidic/basic effects on the properties of ZrO_2 powders produced have been reported for the $NaNO_3$–KNO_3 system by the addition of Lux–Flood bases of Na_2O_2, Na_2CO_3 and $NaNO_2$–KNO_2 [7].

3.3. The purities of the ZrO_2 powders precipitated

The results of chemical analysis, performed by AA, for zirconia powders prepared in different systems, are listed in Table IV. It can be seen that the impurity levels of elemental sodium and potassium in the ZrO_2 powders precipitated in both nitrite and nitrate melts are low, in total both lower than 1.5 wt %. The powders precipitated from the nitrite melt have much lower sodium and potassium impurity levels than the powders prepared in the nitrate melts, either in the $NaNO_3$–KNO_3 eutectic melt or the single $NaNO_3$ solvent. However, there is little difference in the impurity levels of sodium and potassium in the ZrO_2 powders precipitated in the $NaNO_3$–KNO_3 and $NaNO_3$ systems, although they are slightly lower in the $NaNO_3$ system than in the $NaNO_3$–KNO_3 system.

The addition of Na_2O_2 as a Lux–Flood base to the $NaNO_3$–KNO_3 melt did not increase the impurity levels of sodium and potassium in the ZrO_2 powders produced even at concentrations of 20 mol % Na_2O_2. On the contrary, the impurity levels were lowered

TABLE III Preparation of ZrO_2 in nitrate systems

Starting material	Solvent	Temp. (°C)	Time (min)	Phases	Crystallite size (nm)
1 β-$Zr(SO_4)_2$	$LiNO_3$–KNO_3	450	90	m + t[a]	11.4
2 β-$Zr(SO_4)_2$	$NaNO_3$	450	90	m + t	17.1
3 β-$Zr(SO_4)_2$	$NaNO_3$–KNO_3	450 (add at 320 °C)	90	m + t	17.0
4 $Zr(SO_4)_2 \cdot 4H_2O$	$NaNO_3$–KNO_3	450	90	m + t	17.0
5 β-$Zr(SO_4)_2$	$NaNO_3$–KNO_3	450	90	m + t	17.0
6 α-$Zr(SO_4)_2$	$NaNO_3$–KNO_3	300	60	p/a[b]	
7 α-$Zr(SO_4)_2$	$NaNO_3$–KNO_3	400	60	m + t	14.9
8 α-$Zr(SO_4)_2$	$NaNO_3$–KNO_3	450	60	m + t	16.4

[a] m + t: monoclinic + tetragonal.
[b] p/a: poorly crystalline or amorphous.

TABLE IV Chemical analysis results of ZrO_2 precipitated in different nitrite and nitrate systems

Systems	Metal element (wt %)	
	Na	K
$NaNO_2$–KNO_2	0.27 ± 0.01	0.01 ± 0.001
$NaNO_3$–KNO_3	0.87 ± 0.03	0.52 ± 0.02
$NaNO_3$	0.79 ± 0.03	0.46 ± 0.02
$NaNO_3$–KNO_3 + Na_2O_2 (5 mol %)	0.26 ± 0.01	0.07 ± 0.01
$NaNO_3$–KNO_3 + Na_2O_2 (20 mol %)	0.27 ± 0.01	0.02 ± 0.001

TABLE V The settling time and sediment height under different washing conditions

Water		Dilute H_2SO_4		Isopropyl alcohol		Ultrasonic[a]	
Time (h)	Height (mm)	Time (h)	Height (mm)	Time (h)	Height (mm)	Time (h)	Height (mm)
4	70	6	55.5	7	44	> 24	39

[a] Ultrasonic agitation in isopropyl alcohol as the final wash.

significantly and the values were similar to those of the powders prepared in the $NaNO_2$–KNO_2 system.

The basicity of the melt was possibly responsible for the impurity levels of the powders precipitated. The explanation could be proposed that the reaction in the $NaNO_2$–KNO_2 system to form ZrO_2 powders occurred more rapidly and was completed in a single-stage [6]. This would minimize the number of sodium and potassium ions incorporated into the ZrO_2 powders during the reaction. However, the multiple steps and longer duration of the reactions in nitrate systems would allow the sodium and potassium ions more chance to be incorporated into the ZrO_2 powders during the reactions. Because the addition of Na_2O_2 to the $NaNO_3$–KNO_3 melt increased the basicity of the melt, and the reaction rate was also increased, although the concentration of sodium ions in the melt was increased by the same step, the impurity levels in the ZrO_2 powders were lowered, as explained above.

3.4. Processing of the precipitated powders

The precipitated powders were usually washed in distilled water a number of times to dissolve the melt and to separate the powders by means of vacuum filtration, until no anions such as SO_4^{2-}, NO_3^- and NO_2^-, could be detected in the water. Sometimes an ultra-centrifuge was employed to separate the ZrO_2 powders precipitated from the molten salts or separate the ZrO_2 powders from water solution during the washing process. It was found that the separation was accelerated and water washing times were decreased. This may have an effect in preventing the formation of hard agglomerates caused by water.

In order to compare different washing procedures, dilute H_2SO_4, isopropyl alcohol and ultrasonic agitation during water or isopropyl alcohol washing were also employed during the washing process to study their effects on the dispersion and agglomeration of the powders. Table V indicates the particle settling time and heights for these samples in water; these were conducted in a thin glass tube. It is based on the idea that the smaller and well-dispersed particles would take a longer time to settle into a smaller sediment volume, whereas the hard agglomerated particles would settle rapidly into a larger sediment volume. The powders used in these processes were produced by the reaction of β-$Zr(SO_4)_2$ in the $NaNO_2$–KNO_2 system at 450 °C, 90 min in order to make comparison possible.

The water-washed particles settled quickly into the largest sediment volumes of all the samples and in less than 4 h the water became clear, whereas particles washed by dilute H_2SO_4 and isopropyl alcohol took longer to settle (about 6 or 7 h, respectively) and into much smaller sediment volumes. The ultrasonically dispersed particles in the final wash with isopropyl alcohol finished settling in the longest time (over 24 h) into the smallest sediment volumes. The settling time and sediment height were checked when the water became completely clear.

The agglomeration of the powders processed under different washing conditions was examined by TEM. The micrographs obtained are shown in Fig. 5. It can be seen that the degree of particle agglomeration varied significantly in the products processed by means of different washing methods. The water-washed ZrO_2 powders consisted of hard agglomerates and the largest agglomerate was approximately 15 μm diameter. The agglomeration of particles using dilute H_2SO_4 in washing was decreased to a certain degree but there were still some hard agglomerates, whereas the isopropyl alcohol-washed powders exhibited soft agglomeration with primary particle size ranging from 0.6–1.5 μm. Finally, the ultrasonically agitated powders in isopropyl alcohol were very fine and very well dispersed.

The transmission electron micrographs (Fig. 6) at higher magnifications showed details of the crystallite and particle dispersion. Firstly, the water-washed powders were strongly aggregated, forming large powder lumps and it was difficult to see the details of the crystallite. In the alcohol-washed sample, the powder was well dispersed with soft agglomerates. However, in the ultrasonically processed powder in alcohol, some of the macro-crystals were very well dispersed and others were soft agglomerates. It can also be seen from the micrographs of either the alcohol-washed or the ultrasonically processed powders, that the individual crystals were round and uniform, and approximately less than 5 nm in size. This was almost the same as the crystallite size measured by XRD.

These results indicate that hard agglomerates would be formed if just water was used in the washing process. The degree of agglomeration can be reduced by using dilute H_2SO_4 and alcohol washing, especially with the addition of ultrasonic dispersion in alcohol washing.

It has been found that the washing process has very important effects on the formation of agglomerates. Because adhesive forces exist between fine particles,

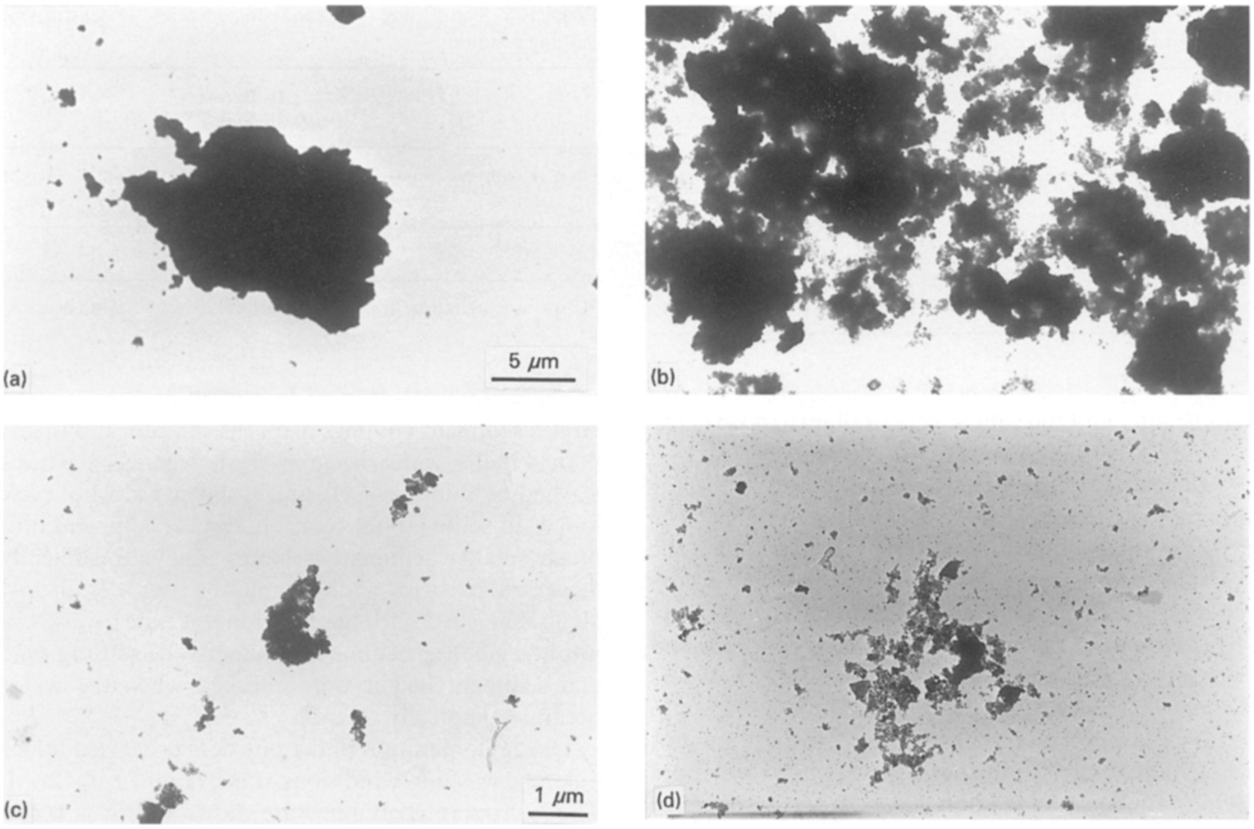

Figure 5 TEM examination of ZrO_2 powders at lower magnifications. (a) Water-washed powder, (b) dilute H_2SO_4-washed powder, (c) alcohol-washed powder, (d) ultrasonically dispersed powder.

agglomeration occurs naturally in powders, due to electrostatic and Van der Waals forces, etc. [8].

There are several possible reasons why the water-washed powders consist of hard agglomerates. Strong hydrogen bonding can be created between the powders. The particles are in close contact as drying of the particles commences. Strong capillary forces could cause significant shrinkage and hardening of the precipitation products during the drying of the particles. With further dehydration, strong bonding between the crystallites and within aggregates can be formed. The hydrogen bonding leads to the formation of actual chemical bonds preferentially between particles. This "bridging" [14, 15] reaction yields hard agglomerates and can be written as

$$\text{Zr–OH} + \text{HO–Zr} \rightarrow \text{Zr–O–Zr} + H_2O \quad (1)$$

Dilute H_2SO_4 washing does not prevent the water effects of agglomeration, because after dilute H_2SO_4 washing, water has to be employed to eliminate SO_4^{2-} in the solution. Using dilute H_2SO_4, however, may affect the dissolution of the molten salt. The latter can cause small particles to join together, so that the use of dilute H_2SO_4 may enhance the dispersion of the powders.

By replacing water with alcohol, the strong bridging hydroxyl groups and the coordinated water can be removed, which ultimately prevents the formation of hard agglomerates by inhibiting the condensation reaction (Reaction 1). This results in the formation of alkoxy groups which provide the basis for agglomeration control in powders. The different mechanisms of washing with water and alcohol were proposed by Kaliszewski and Heuer [14].

Ultrasonic agitation has been found to be very effective in facilitating the deaggregation and dispersion of the particles in solutions [16]. If the ultrasonic agitation and alcohol washing are combined together, very well-dispersed powders can be obtained (Fig. 6c).

4. Conclusion

Very fine zirconia powders can be prepared by the reaction of zirconium sulphate in various molten nitrite and nitrate solvents in the temperature range 200–600 °C.

The ZrO_2 powders precipitated in the $NaNO_2$–KNO_2 system are all of the tetragonal phase, regardless of whether anhydrous α-$Zr(SO_4)_2$ or β-$Zr(SO_4)_2$ was used as the starting material. In addition to this, there are no differences in either crystallite size or structure when α-$Zr(SO_4)_2$ or β-$Zr(SO_4)_2$ is used as the starting material.

The ZrO_2 powders produced in nitrate systems, including $LiNO_3$–KNO_3 and $NaNO_3$–KNO_3 eutectics and $NaNO_3$ single melt, are all a mixture of the monoclinic and tetragonal phases with crystallite sizes between 10 and 20 nm, whereas the tetragonal structure of ZrO_2 precipitated in the $NaNO_2$–KNO_2 system is very fine with the crystallite size less than 10 nm. The impurity levels of sodium and potassium in powders prepared from the $NaNO_2$–KNO_2 system are also lower than those from nitrate melts.

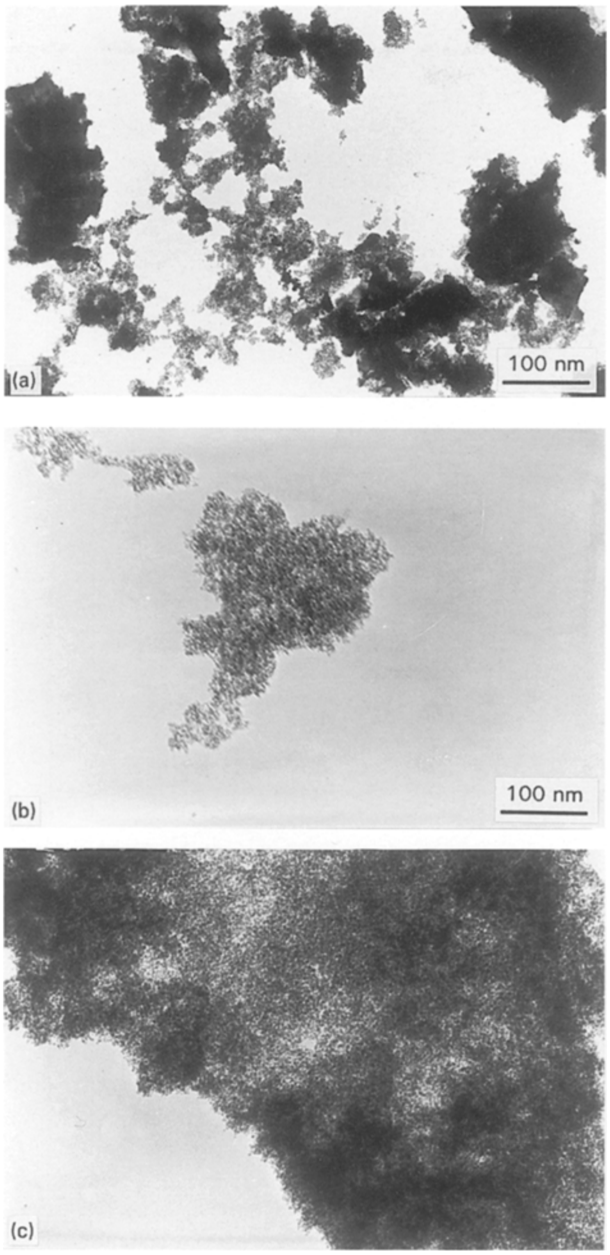

Figure 6 TEM examination of ZrO_2 powders at higher magnifications. (a) Water-washed powder, (b) alcohol-washed powder, (c) ultrasonically dispersed powder.

The crystallite size of ZrO_2 powders precipitated in both nitrites and nitrates increases with increase of reaction temperature and time.

Good particle distribution with soft agglomeration can be obtained when ultrasound agitation is employed in the process of washing the ZrO_2 powders. Soft agglomerates can also be observed after the powders are alcohol washed and dried. The use of dilute H_2SO_4 during the washing process has the effect of breaking down some of the aggregates. However, hard agglomerates were produced if the precipitates were only water washed and dried.

References

1. B. DURAND and M. ROUBIN, *Mater. Sci. Forum* **73–75** (1991) 663.
2. M. JEBROUNI, B. DURAND and M. ROUBIN, *Ann. Chim. Fr.* **16** (1991) 569.
3. D. H. KERRIDGE and J. CANCELA REY, *J. Inorg. Nucl. Chem.* **39** (1977) 405.
4. C. B. FINCH and P. F. BELCHER, *J. Cryst. Growth* **60** (1982) 321.
5. H. AL-RAIHANI, B. DURAND, F. CHASSAGNEUX, D. H. KERRIDGE and D. INMAN, *J. Mater. Chem.* **4** (1994) 1331.
6. Y. DU and D. INMAN, *ibid.* **5** (1995) 1927.
7. Y. DU, P. ROGERS and D. INMAN, *J. Mater. Sci.* (1996) **31** (1996) 3361.
8. H. RAMPF and H. SCHUBERT, in "Ceramic Processing before Firing", edited by G. Y. Onoda Jr and L. L. Hench (Wiley, New York, 1978) p. 61.
9. I. J. BEAR, *Aust. J. Chem.* **19** (1966) 357.
10. I. J. BEAR and G. M. LUKASZEWSKI, *ibid.* **19** (1966) 1973.
11. I. J. BEAR, *ibid.* **20** (1967) 415.
12. G. CHARLOT, "Qualitative Inorganic Analysis" (Methuen, London, 1957) p. 296.
13. H. P. KLUG and L. E. ALEXANDER, "X-ray Diffraction Procedure", 2nd Edn (Wiley, New York, 1974) Ch. 9.
14. M. S. KALISZEWSKI and A. H. HEUER, *J. Am Ceram. Soc.* **73** (1990) 1504.
15. S. L. JONES and J. S. NORMAN, *ibid.* **71** (1988) C-190.
16. E. JORGE and T. CHARTIER, *ibid.* **73** (1990) 2552.

Received 6 February
and accepted 18 March 1996